Published in final edited form as:

Science. 2013 January 11; 339(6116): 204–207. doi:10.1126/science.1229326.

Ezh2 orchestrates topographic tangential migration and connectivity of mouse precerebellar neurons

Thomas Di Meglio[1,*], **Claudius F. Kratochwil**[1,2,*], **Nathalie Vilain**[1], **Alberto Loche**[1,2], **Antonio Vitobello**[1,2], **Keisuke Yonehara**[1], **Steven M. Hrycaj**[3], **Botond Roska**[1,2], **Antoine H.F.M. Peters**[1,2], **Anne Eichmann**[3], **Deneen Wellik**[4], **Sebastien Ducret**[1], and **Filippo M. Rijli**[1,2,†]

[1]Friedrich Miescher Institute for Biomedical Research, Maulbeerstrasse 66, 4058 Basel, Switzerland [2]University of Basel, 4056 Basel, Switzerland [3]Yale Cardiovascular Research Center, Department of Internal Medicine, Yale University School of Medicine, New Haven, CT 06511-6664, USA [4]Department of Cell and Developmental Biology, University of Michigan, Ann Arbor, MI 48109-2200, USA

Abstract

We investigated the role of histone methyltransferase *Ezh2* in tangential migration of mouse precerebellar pontine nuclei, the main relay between neocortex and cerebellum. By counteracting the sonic hedgehog pathway, *Ezh2* represses *Netrin1* in dorsal hindbrain allowing normal pontine neuron migration. In *Ezh2* mutants, ectopic *Netrin1* derepression results in abnormal migration and supernumerary nuclei integrating brain circuitry. Moreover, intrinsic topographic organization of pontine nuclei according to rostrocaudal progenitor origin is maintained throughout migration and correlates with patterned cortical input. *Ezh2* maintains spatially-restricted *Hox* expression which in turn regulates differential expression of the repulsive receptor *Unc5b* in migrating neurons, generating subsets with distinct responsiveness to environmental *Netrin1*. Thus, *Ezh2*-dependent epigenetic regulation of intrinsic and extrinsic transcriptional programs controls topographic neuronal guidance and connectivity in the cortico-ponto-cerebellar pathway.

In mammals, cortical motor and sensory information is mostly relayed to the cerebellum via the hindbrain precerebellar pontine nuclei (PN), which include pontine gray and reticulotegmental nuclei. The developing hindbrain is rostrocaudally segregated into progenitor compartments, or rhombomeres (r1–r8) (1), genetically defined by nested *Hox* gene expression (2). Mouse PN neurons are generated from r6–r8 lower rhombic lip progenitors (3), undergo a long-distance caudorostral tangential migration via the anterior extramural stream (AES), and settle beside the ventral midline (Fig. 1, A and B) (4, 5). Intrinsic expression of transcription factors and guidance receptors and extrinsic distribution

[†]To whom correspondence should be addressed: filippo.rijli@fmi.ch.
[*]These authors contributed equally to this work

Supporting Online Material

www.sciencemag.org/cgi/content/full/science.1229326/DC1
Materials and Methods
Figs. S1 to S10
References (18–37)

of ligands are important for AES migration (6–8). However, little is known about the epigenetic regulation of these transcriptional programs. Here, we addressed the role of *Ezh2*, which is member of the Polycomb Repressive Complex 2 and trimethylates histone H3 at Lysine 27 (H3K27me3) (9).

Ezh2 transcripts are maintained through late stages in lower rhombic lip progenitors, migratory stream and PN neurons (fig. S1), while H3K27m3 is detected throughout the hindbrain (fig. S2). To conditionally inactivate *Ezh2*, we generated transgenic lines in which *Cre* is driven by rhombomere-specific enhancers in spatially-restricted regions tiling the caudal hindbrain ((10), figs. S3 and S4). To assess cell-autonomous and/or region-specific non-cell-autonomous *Ezh2* function in pontine neuron migration, we first crossed *Krox20::Cre* (10) to an $Ezh2^{fl/fl}$ allele (10) ($Krox20::Cre;Ezh2^{fl/fl}$). Inactivation in r3 and r5, which do not contribute to the pontine migratory stream (3), resulted in small ectopic pontine nuclei in posterior r5 (PN^e, fig. S5), supporting an *Ezh2* non-cell-autonomous role. Deletion in r5 and r6 ($r5–6::Cre;Ezh2^{fl/fl}$) resulted in a more prominent phenotype. A neuronal subset split from the migratory stream, turned ventrally, and generated an ectopic duplication of PN (PN^e) (Fig. 1, E to G). PN^e neurons were non-recombined $Ezh2^{+/+}$ $H3K27me3^+$ located within the r5–r6-derived territory mostly devoid of H3K27me3 (fig. S2), further confirming *Ezh2* non-cell-autonomous function.

To assess whether ectopic PN^e integrated cortico-cerebellar connectivity, we carried out cortex-to-PN and cerebellum-to-PN tracings. We injected viral constructs expressing GFP (Rabies-ΔG-GFP) and/or mCherry (Rabies-ΔG-mCherry) in P2 wild type, $r5–6::Cre;Ezh2^{fl/fl}$, and $Krox20::Cre;Ezh2^{fl/fl}$ mutants. At P7, PN and PN^e triggered collateralization of corticospinal axons and innervated the cerebellum (Fig. 1, C and H, fig. S6).

To evaluate *Ezh2* cell-autonomous function, we used the *Wnt1::Cre* deleter (10). *Ezh2* transcripts and H3K27me3 were selectively deleted from lower rhombic lip and migratory stream in $Wnt1::Cre;Ezh2^{fl/fl}$ mutants (fig. S2 and S7). Nonetheless, the mutation was not sufficient to induce ectopic posterior pontine neuron migration (Fig. 2, J and M, figs. S5 and S7). The most severe phenotype was observed in $Hoxa2::Cre;Ezh2^{fl/fl}$ mutants, where *Ezh2* was inactivated in both AES neurons and their migratory environment, i.e. throughout r3–r6 and dorsal r7–8 derived structures including the lower rhombic lip (figs. S2 and S3). The whole AES did not migrate anterior to r6 and settled into a single posterior ectopic nucleus (PN^e, fig. S5). Thus, *Ezh2* has a non-cell-autonomous role in AES migration, which is enhanced by a cell-autonomous function in progenitors and migrating neurons.

Netrin1 (Ntn1) and Slit1-3 are attractive/repulsive secreted cues that influence pontine neuron migration (6, 7). While *Slit1-3* expression was not altered in E14.5 $r5–6::Cre;Ezh2^{fl/fl}$ mutants (fig. S8), *Ntn1*, normally expressed in floor-plate and ventral ventricular progenitors (Fig. 1D, fig. S5) (11), was ectopically expressed in dorsal progenitors and mantle layer medially to the AES in $r5–6::Cre;Ezh2^{fl/fl}$, $Krox20::Cre;Ezh2^{fl/fl}$, $Hoxa2::Cre;Ezh2^{fl/fl}$ and $r5post::Cre;Ezh2^{fl/fl}$ mutants (Fig. 1I, fig. S5). Additional deletion of *Shh* was sufficient to prevent strong ectopic *Ntn1* activation in dorsal progenitors of E12.5 $r5post::Cre;Ezh2^{fl/fl};Shh^{fl/fl}$ conditional mutants (fig. S5). At

E14.5, ectopic *Ntn1* was almost undetectable partially rescuing the *Ezh2* knockout (Fig. 1, J and K, fig. S5). Therefore, *Ezh2* is required to restrict *Ntn1* expression to ventral progenitors by silencing *Ntn1* in dorsal neural tube. However, *Ezh2* deletion is not sufficient to ectopically induce *Ntn1*, which additionally requires Shh signaling from the floor plate. Thus, in the dorsal neural tube, *Ezh2*-mediated epigenetic repression of *Ntn1* may normally counteract Shh-mediated activation.

Ectopic and/or increased environmental Ntn1 levels may trigger premature migration towards the midline. In E14.5 *r5–6::Cre;Ezh2*$^{fl/fl}$ mutants, only a subset of pontine neurons split from the stream and entered the alternative ventral migratory pathway at the level of the ectopic *Ntn1*$^{+}$ domain (Fig. 1I, fig. S5), suggesting that AES neurons may display intrinsic differential responsiveness to Ntn1 signaling. To fate map the contributions of r6 (*r6RL*^{P}) or r7–8 (*r7-8RL*^{P}) lower rhombic lip-derived neuronal progenies into the pontine stream and nuclei (Fig. 2, B, C and H, fig. S3), we crossed floxed reporter lines to *r5–6::Cre* or *r7post::Cre* (*Cre* is expressed up to the r6/r7 boundary; fig. S3H) in which *Cre* is down-regulated before AES migration (fig. S4). *r6RL*^{P} mapping was confirmed by the tamoxifen-inducible *MafB::CreERT2* transgenic line, whose reporter expression pattern is restricted to r5–r6, similar to *r5–6::Cre* (10, fig. S3). To trace the whole precerebellar lower rhombic lip progeny (*r6-8RL*^{p}), we used *r5post::Cre* (figs. S3A and S4).

r6-8RL^{p} contributed to the whole pontine nuclei (fig. S3), whereas *r6RL*^{P} mapped to the most anterior (arrow; Fig. 2H, fig. S3), and *r7-8RL*^{p} filled the remaining posterior portions of pontine nuclei (fig. S3). This topographic organization of pontine neuronal subsets directly correlated with their relative position within the migratory stream. Namely, *r6RL*^{p} mapped to the dorsalmost AES, whereas *r7-8RL*^{p} contributed to the remaining portion ventrally to *r6RL*^{p} (Fig. 2, B and C). Thus, the precerebellar lower rhombic lip is rostrocaudally mapped onto the AES dorsoventral axis (Fig. 3E, fig. S1J) and, in turn, onto the PN rostrocaudal axis (fig. S1K), with neuronal subsets maintaining their relative position throughout migration and settling.

Next, we investigated molecular correlates of this intrinsic cellular regionalization and asked whether *Hox* paralog group (PG)2–5 maintain their spatially-restricted progenitor expression patterns in pontine migratory stream and nuclei (Fig. 2). Indeed, *Hox* PG2 (*Hoxa2*/*Hoxb2*) and PG3 (*Hoxa3*/*Hoxb3*), expressed in the whole precerebellar rhombic lip, were correspondingly maintained throughout the pontine migratory stream and nuclei (6) (fig. S1). *Hoxb4* is normally expressed up to the r6/r7 boundary, whereas the *Hox PG5* rostral expression limit is posterior to *PG4* genes (2). In the AES and PN, Hoxb4^{+} neurons extended just ventrally and posteriorly, respectively, to *r6RL*^{P} (Fig. 2, C and D, fig. S1L), whereas *Hoxa5* and *Hoxb5* transcripts and Hoxa5 protein mapped to the ventralmost migratory stream and posteriormost pontine nuclei, respectively (Fig. 2A, F, H and I, fig. S1 and S2). Simultaneous detection of Hoxa5 and ZsGreen in *r5–6::Cre;R26R*^{ZsGreen} specimen demonstrated rostrocaudal segregation of *r6RL*^{p} and Hoxa5^{+} neurons within the pontine nuclei (Fig. 2H). To permanently label *Hoxa5*-expressing neurons, we generated a transgenic line in which *Cre* was inserted in-frame at the *Hoxa5* locus (*Hoxa5::Cre*) (10) (fig. S3). *Hoxa5::Cre*-expressing neurons segregated to the ventralmost AES and posteriormost PN, faithfully overlapping endogenous Hoxa5 distribution (Fig. 2, D, E, F and G, figs. S1F, S3

and S4). Thus, pontine neuron subsets of distinct rostrocaudal origin maintain their relative topographic positions and *Hox* codes throughout migration and settling within the target nucleus (Fig. 4A, fig. S1).

Is *Ezh2* required to maintain *Hox* nested expression in migrating pontine neurons and nuclei? In E14.5 *Wnt1::Cre;Ezh2$^{fl/fl}$* and *Hoxa2::Cre;Ezh2$^{fl/fl}$* mutants, Hoxb4, Hoxa5 and *Hoxb5* were ectopically expressed within the anterior lower rhombic lip and spread ventrodorsally throughout the pontine migratory stream (Fig. 2, L and M, figs. S2 and S7). Thus, by preventing *Hox PG4* and *PG5* expression in anterior precerebellar rhombic lip and migrating neuronal progeny, *Ezh2*-mediated repression contributes to the maintenance of molecular heterogeneity in the migratory stream. This, in turn, may underlie intrinsic differential response of migrating neuron subsets to environmental Ntn1.

Netrin-mediated attraction is counteracted by Unc5 repulsive receptors (12) and *Unc5c* inactivation results in variable ectopic migration of AES neurons (13). *Unc5c* is expressed in lower rhombic lip progenitors, downregulated in migrating neurons, and reactivated upon approaching the midline (fig. S9) (13). Thus, *Unc5c* is unlikely to confer dorsoventrally biased response of the AES to Ntn1. *Unc5b* has been involved in vascular development (14), though a role in neuronal development was not explored. We found a dorsoventral high-to-low density of cells expressing *Unc5b* (Fig. 3C, fig. S9), and b-galactosidase activity in *Unc5b$^{bGal/+}$* fetuses (Fig. 3A). *Unc5b* expression was in turn downregulated upon the migratory stream turning towards the midline (fig. S9C). Dorsoventral *Unc5b* transcript distribution in the migratory stream anti-correlated with *Hox PG5* expression (Fig. 3, C and D). In E14.5 *Hoxa5$^{-/-}$;Hoxb5$^{-/-}$;Hoxc5$^{-/-}$* compound mutants, *Unc5b* was up-regulated in ventral Hoxb4^{+}/Pax6^{+} AES neurons (Fig. 3, H and I). Thus, Hox PG5 normally represses *Unc5b* in ventral AES neurons originating from posterior precerebellar lower rhombic lip.

In E14.5 *Unc5b$^{bGal/bGal}$* null mutants, β-galactosidase^{+} cells partially lost their normal dorsal restriction and spread into ventral AES (Fig. 3B). Thus, *Unc5b* contributes to maintain topographical organization of dorsal AES subsets. In E16.5 *Unc5c$^{-/-}$* fetuses, dorsal *Unc5b* expressing AES neurons maintained their normal migratory path, whereas ectopic neurons were *Hox PG5^{+}* and mainly *Unc5b*-negative (fig. S9). Therefore, in the absence of *Unc5c*, ventral *Unc5b*-negative AES neurons become more sensitive to Ntn1-mediated attraction than dorsal *Unc5b*-expressing neurons. Similarly, in *r5–6::Cre;Ezh2$^{fl/fl}$* mutants, *Unc5b* expressing neurons remain dorsal and pursue their normal migration, whereas *Hox PG5^{+}*/*Unc5b*-negative neurons are preferentially influenced by Ntn1 upregulation and ectopically attracted to the midline (Fig. 3, F and G, fig. S2). Moreover, in *Hoxa2::Cre;Ezh2$^{fl/fl}$* mutants, in which all pontine neurons are *Ezh2$^{-/-}$*/H3K27me3^{-} and migrate through an environment ectopically expressing *Ntn1* (fig. S5), all migrating neurons are prematurely attracted to an ectopic posterior midline position, are *Hox PG5^{+}*, and down-regulate *Unc5b* (figs. S2 and S7).

Next, *Unc5b/5c* overexpression by *in utero* electroporation of E14.5 lower rhombic lip progenitors was sufficient to cell-autonomously rescue the PN^{e} phenotype in *r5–6::Cre;Ezh2$^{fl/fl}$* mutants (eGFP^{+} neuron quantification in PN^{e} compared to PN: eGFP (n=5) 33.79%±0.1060; eGFP/Unc5b/5c (n=5) 0.64%±0.0044; p=0.00011) (Fig. 3, J and K),

demonstrating that elevating Unc5 receptor levels counteracts increased Ntn1-mediated attraction. Ntn1 overexpression by electroporation in E13.5 wild type fetuses induced ectopic posterior migration of AES neurons (Fig. 3L), partially phenocopying the *r5–6::Cre;Ezh2*$^{fl/fl}$ mutant phenotype, showing that increasing Ntn1 is sufficient to cause ectopic ventral migration of neuronal subsets.

Furthermore, while overexpression of *Unc5c* in E13.5 wild type fetuses had no apparent effect on AES migration (Fig. 3, M and N), *Unc5b* electroporation triggered ectopic anterior migration and/or block in dorsal position of Hoxa5-negative pontine neurons subsets (Fig. 3, O to Q). Therefore, maintaining constitutively high Unc5b levels in migrating neurons prevents or delays turning towards the midline, the latter resulting in ectopic anterior migration. Conditional *Hoxa2* overexpression in rhombic lip derivatives by mating *Wnt1::Cre* with a *ROSA26::(lox-STOP-lox)Hoxa2-IRES-EGFP* (*Wnt1::Cre;R26R*^{Hoxa2}) (10) allele also resulted in anterior ectopic migration generating rostrally elongated pontine nuclei, which maintained high *Unc5b* expression, unlike in controls (fig. S9). Therefore, while *Hox PG5* are involved in negatively regulating *Unc5b* in the ventral migratory stream, *Unc5b* expression in dorsal AES may be under *Hox PG2* positive regulation generating differential responses to environmental Ntn1.

Finally, we investigated whether the PN and PN^{e} patterning differences in *r5–6::Cre;Ezh2*$^{fl/fl}$ mutants result in distinct cortical inputs. In P7 *Pcp2::Cre;R26R*^{tdTomato} animals (10) expressing *Cre* in medio-posterior (including visual) cortex (MPC), *tdTomato*$^{+}$ axons projected onto the rostral pontine nuclei, in agreement with (15), including the *r6RL*^{p} neuron subset (fig. S6). Co-injection of rabies-ΔG-GFP and rabies-ΔG-mCherry into visual/MPC and medial somatosensory cortex (SSC) resulted in rostral GFP^{+} and caudal mCherry^{+} axonal inputs onto the pontine nuclei, respectively (Fig. 4C). In *r5–6::Cre;Ezh2*$^{fl/fl}$ mutants, PN was targeted both by visual/MPC-derived GFP^{+} (rostrally) and SSC-derived mCherry^{+} (caudally) axons, whereas PN^{e} was innervated by SSC-derived though not visual/MPC-derived axons (Fig. 4G), correlating with their posterior *Hox PG5*$^{+}$ profile (Fig. 4, A, B and D to F).

During radial migration, correlation to rostrocaudal position of origin is maintained through interaction with glial progenitors (16). How long-range tangentially migrating neurons (17) maintain information about their origin is less understood. We show that the topographic migratory program of r6–r8 derived pontine neurons is largely established in progenitor pools according to rostrocaudal origin and maintained in migrating neurons. We found similar organizational principles during lateral reticular nucleus migration (fig. S10). Moreover, the r2–r5 rhombic lip also gives rise to neurons that migrate tangentially along a short dorsoventral extramural path and populate distinct brainstem cochlear nuclei with a rostrocaudal topography (3). On its caudorostral route, the precerebellar stream migrates ventrally to the cochlear stream (3) though they do not mix despite close cellular proximity, suggesting that rhombomere-specific programs may control appropriate precerebellar neuron position during tangential migration. Indeed, we show that the topography of r6- versus r7- versus r8-origin is preserved throughout migration, mapped along the dorsoventral axis of the pontine stream and eventually within rostrocaudal subregions of the pontine nuclei, correlating with patterned cortical input. The transcriptional regulation of this tangential

migratory program is epigenetically maintained (Fig. 4H). *Ezh2*-mediated repression maintains dorsoventrally-restricted environmental distribution of attractive/repulsive cues such as *Ntn1* and an intrinsically heterogeneous *Hox* transcriptional program in the migratory stream that, in turn, provides neuronal subsets with distinct Unc5b-dependent responses to environmental Ntn1, thus contributing to maintain neuronal position during migration.

Supplementary Material

Refer to Web version on PubMed Central for supplementary material.

Acknowledgments

We thank K. Balint, F. Boukhtouche, Y.-Y. Lee, C.-Y. Liang, D. Kraus, T. Mathivet, F. Santagati, J.F. Spetz, A. Yallowitz, for technical support and discussion. We are grateful to M. Tessier-Lavigne, S.H. Orkin, E. Callaway, V. Castellani, P. Mehlen, O. Nyabi, J. Haigh for gift of mouse lines, probes, or reagents. T.D. is recipient of an EMBO Long-Term Fellowship. Work in FMR laboratory is supported by the Swiss National Science Foundation (Sinergia CRSI33_127440), ARSEP, and the Novartis Research Foundation.

References and Notes

1. Lumsden A, Krumlauf R. Science. 1996; 274:1109–1115. [PubMed: 8895453]
2. Tümpel S, Wiedemann LM, Krumlauf R. Curr Top Dev Biol. 2009; 88:103–137. [PubMed: 19651303]
3. Farago AF, Awatramani RB, Dymecki SM. Neuron. 2006; 50:205–218. [PubMed: 16630833]
4. Altman J, Bayer SA. J Comp Neurol. 1987; 257:529–552. [PubMed: 3693597]
5. Rodriguez CI, Dymecki SM. Neuron. 2000; 27:475–486. [PubMed: 11055431]
6. Geisen MJ, et al. PLoS Biol. 2008; 6:e142. [PubMed: 18547144]
7. Yee KT, Simon HH, Tessier-Lavigne M, O'Leary DM. Neuron. 1999; 24:607–622. [PubMed: 10595513]
8. Nóbrega-Pereira S, Marín O. Cerebral Cortex. 2009; 19:i107–i113. [PubMed: 19357392]
9. Margueron R, Reinberg D. Nature. 2011; 469:343–349. [PubMed: 21248841]
10. Materials and methods are available as supplementary material on Science Online.
11. Bloch-Gallego E, Ezan F, Tessier-Lavigne M, Sotelo C. J Neurosci. 1999; 19:4407–4420. [PubMed: 10341242]
12. Hong K, et al. Cell. 1999; 97:927–941. [PubMed: 10399920]
13. Kim D, Ackerman SL. J Neurosci. 2011; 31:2167–2179. [PubMed: 21307253]
14. Lu X, et al. Nature. 2004; 432:179–186. [PubMed: 15510105]
15. Leergaard TB, Bjaalie JG. Frontiers in neuroscience. 2007; 1:211–223. [PubMed: 18982130]
16. Rakic P. Science. 1988; 241:170–176. [PubMed: 3291116]
17. Hatten ME. Annu Rev Neurosci. 1999; 22:511–539. [PubMed: 10202547]

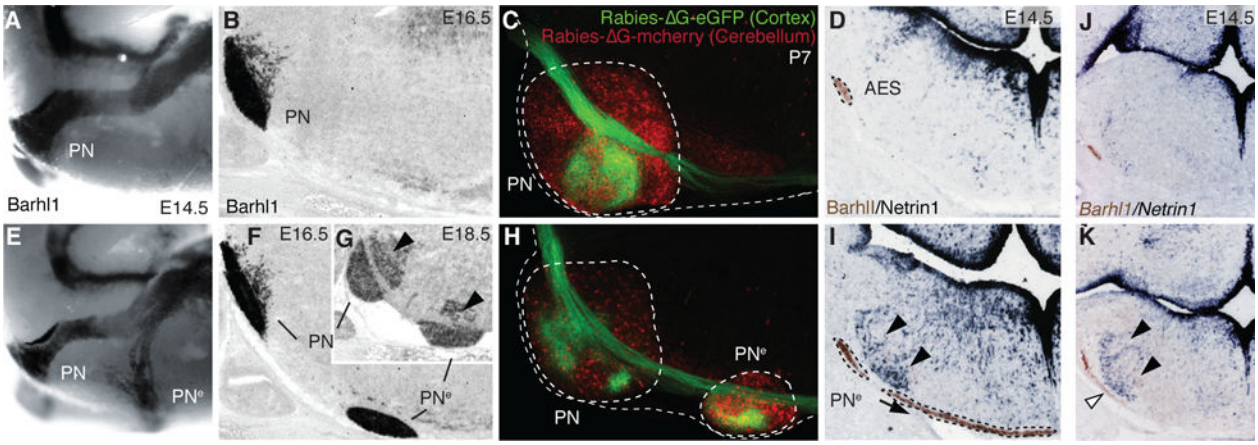

Fig. 1. ***Ezh2*** **non-cell autonomous role in pontine neuron tangential migration**

(**A**, **B, E, F** and **G**) Migratory phenotypes in control (A,B) and *r5–6::Cre;Ezh2*$^{fl/fl}$ mutants (E–G). *Barhl1 in situ* hybridization in E14.5 whole-mount (A,E), and E16.5 (B,F), E18.5 (G) sagittal sections. Pontine gray and reticulotegmental (arrowheads, G) nuclei (PN) are duplicated (PN^{e}). (**C** and **H**) Tracings from P7 cortex (Rabies-ΔG-eGFP) and cerebellum (Rabies-ΔG-mCherry) in controls (C) and *r5–6::Cre;Ezh2*$^{fl/fl}$ mutants (H). Pontine (PN) and ectopic (PN^{e}) nuclei are connected to cortex and cerebellum. (**D, I**, **J** and **K**) *Barlh1*/*Netrin1* expression in E14.5 control (D), *r5–6::Cre;Ezh2*$^{fl/fl}$ (I), *r5post::Cre;Ezh2*$^{fl/fl}$*;Shh*$^{fl/+}$ (K), *r5post::Cre;Ezh2*$^{fl/fl}$*;Shh*$^{fl/fl}$ (J) coronal sections. Ectopic *Ntn1* (arrowheads,I,K) and PN^{e} ectopic migration (arrows,I,K) are partially rescued (J).

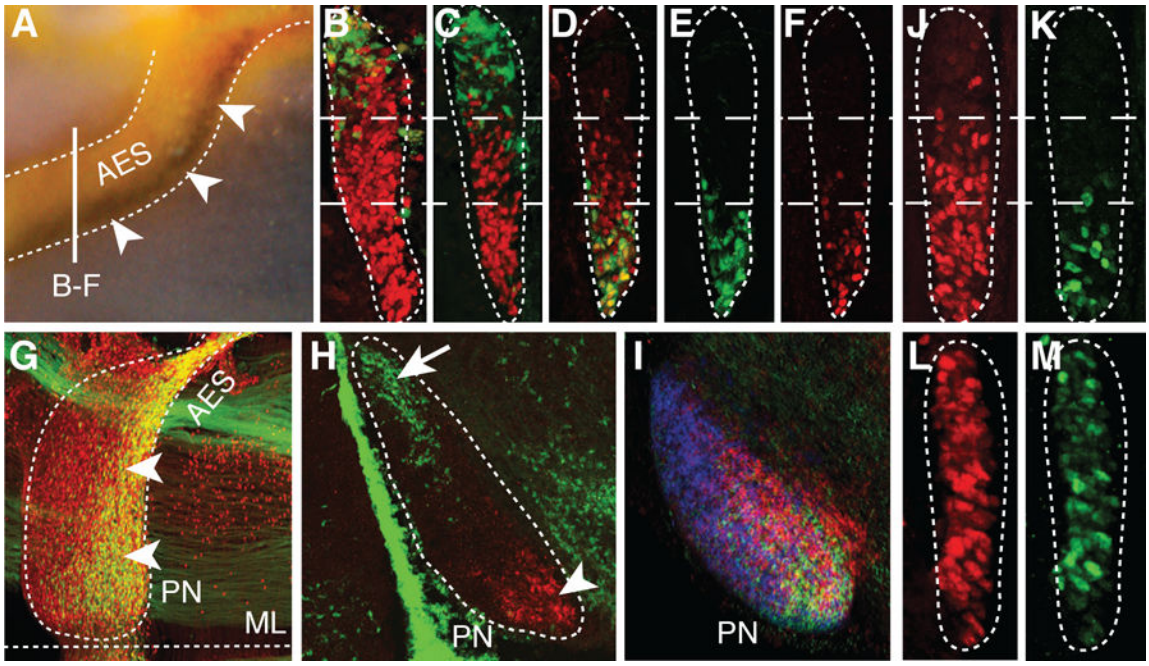

Fig. 2. Intrinsic topography of pontine migratory stream and nuclei and *Ezh2* dependent *Hox* regulation

(**A**) *Hoxb5/Barhl1 in situ* hybridization on E15.5 whole-mount brain (lateral view). Arrowheads show Hoxb5^{+} neuron ventral restriction in anterior extramural stream (AES). (**B** to **C**) E15.5 *r5–6::Cre;R26R^{ZsGreen}* AES coronal sections co-stained with ZsGreen/Pax6 (red) (B) or ZsGreen/Hoxb4 (red) (C) showing complementary dorsal ZsGreen^{+}/ventral Hoxb4^{+} cell distributions (bar in (A) shows section level). (**D** to **F**) E15.5 *Hoxa5::Cre;R26R^{ZsGreen}* AES sections showing partially overlapping ZsGreen/Hoxb4 (red) co-stainings with offset dorsal limits (D), while ZsGreen^{+} (E) and Hoxa5^{+} (F) neurons display similar ventral restriction. (**G** to **H**) E15.5 whole-mount *Hoxa5::Cre;R26R^{ZsGreen}* (G) or *r5–6::Cre;R26R^{ZsGreen}* (H) sagittal sections co-stained with ZsGreen/Pax6 (red) or ZsGreen/Hoxa5 (red), respectively, illustrating posterior pontine nuclei (PN) restriction of Hoxa5^{+} neurons (arrowheads, G,H), and anterior restriction of r6-derived neurons (arrow, H). (**I**) *Hoxb3/Hoxb4/Hoxb5* nested *in situ* expression patterns on PN sagittal section (**J** to **M)** Hoxb4 (red) and Hoxa5 (green) immunostainings of E15.5 *Wnt1::Cre;Ezh2$^{fl/+}$* control (J,K) and *Wnt1::Cre;Ezh2$^{fl/fl}$* mutant (L,M) AES. In (L,M), Hoxb4 and Hoxa5 loose their spatial restriction and are ectopically derepressed up to the dorsal edge of the AES. ML, ventral midline.

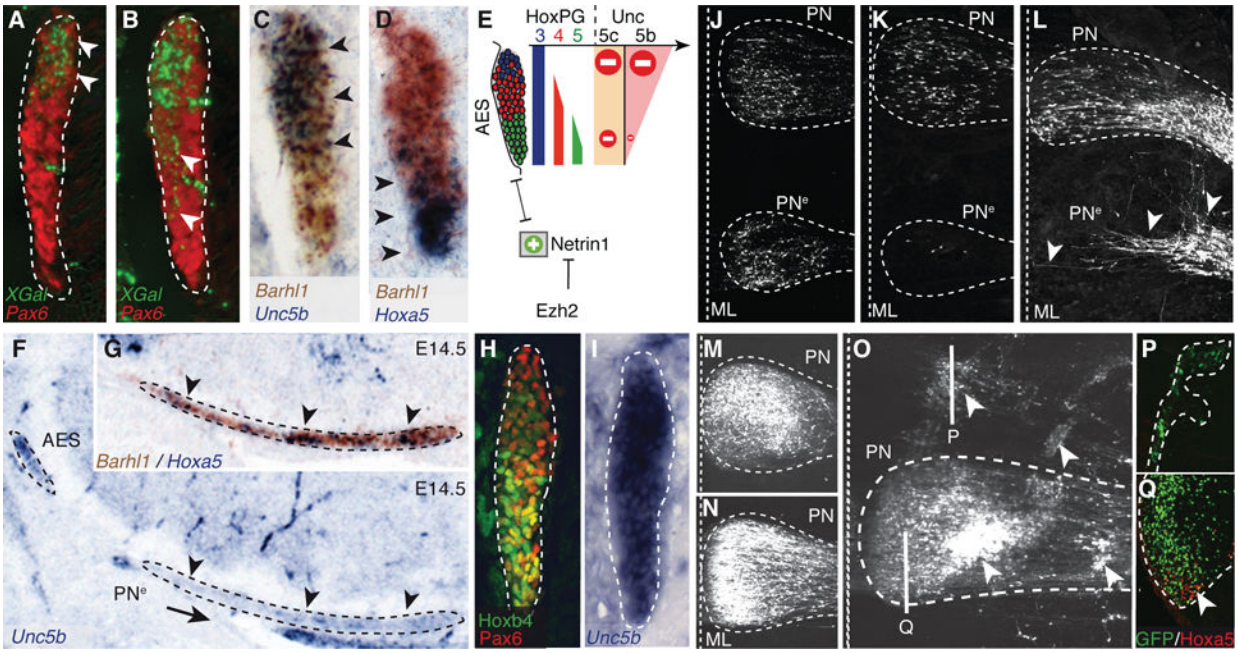

Fig. 3. *Ezh2* and *Hox* dependent regulation of *Unc5b* in pontine neuron migration

(**A** to **B**) X-gal (green)/Pax6 (red) co-stainings of E14.5 *Unc5b*$^{bGal/+}$ heterozygotes (A) and *Unc5b*$^{bGal/bGal}$ homozygotes (B) showing X-gal-stained cell distribution in anterior extramural stream (AES) (arrowheads). (**C** to **E)** *Unc5b*/*Barhl1* (C) and *Hoxa5*/*Barhl1* (D) *in situ* hybridization in E14.5 AES showing complementary dorsoventral expression of *Unc5b* and *Hoxa5* (arrowheads) and summary (E). (**F** to **G**) In *r5–6::Cre;Ezh2*$^{fl/fl}$ mutants, ectopic pontine nuclei (PN^{e}) migrating neurons are *Unc5b*-negative (F) and *Hoxa5*$^{+}$/*Barhl1*$^{+}$ (G) (arrowheads). (**H** to **I)** In E14.5 *Hoxa5*$^{-/-}$/*Hoxb5*$^{-/-}$/*Hoxc5*$^{-/-}$ AES, *Unc5b* is up-regulated ventrally (I), while Hoxb4/Pax6 are normally expressed (H). (**J** to **K)** In utero electroporation (EP) in E14.5 *r5–6::Cre;Ezh2*$^{fl/fl}$ mutants of Unc5b/Unc5c/eGFP strongly reduces at E18.5 ectopically migrating PN^{e} neurons (K), as compared to EP of eGFP (J), partially rescuing the phenotype. (**L** to **Q**) In E13.5 wild type, EP of *Ntn1* results in posterior ectopic pontine neuron migration at E17.5, phenocopying *r5–6::Cre;Ezh2*$^{fl/fl}$ mutants (arrowheads, L). While EP at E13.5 of *eGFP* (M) or *Unc5c/eGFP* has no apparent effect on migration at E18.5 (N), EP of *Unc5b/eGFP* results in anterior ectopic migration and/or dorsal-lateral arrest (arrowheads, O). Immunostaining on sagittal sections shows that anterior ectopic GFP+/Unc5b^{+} electroporated cells are Hoxa5-negative (P); Hoxa5^{+} cells are normally restricted in posterior PN (Q).

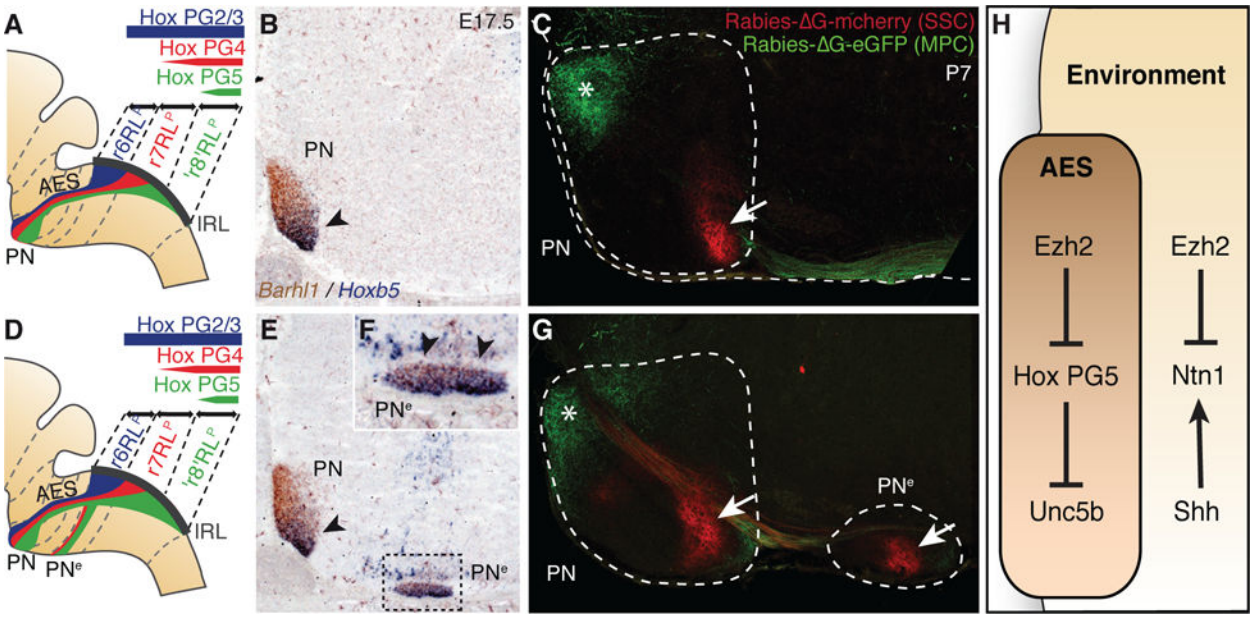

Fig. 4. Pontine nuclei regionalization and patterned cortical input

(**A**, **B**, **D, E** and **F)**, *Hox* expression summary in migrating pontine neurons of control (A) and *r5–6::Cre;Ezh2*$^{fl/fl}$ mutants (D). *Barhl1/Hoxb5 in situ* hybridization on E17.5 sagittal sections (B,E,F). In *r5–6::Cre;Ezh2*$^{fl/fl}$ mutants (E,F), Hoxb5^{+} neurons spread throughout the rostrocaudal extent of the ectopic nucleus (PN^{e}) (arrowheads, F), while in PN they are normally posteriorly restricted as in control (arrowhead, B,E). (**C** and **G**) Rabies-ΔG viruses injected in control visual/medioposterior (MPC) and somatosensory (SSC) cortex anterogradely trace fibers into anterior (green,*) and posterior (red, arrow) PN (C), respectively. In *r5–6::Cre;Ezh2*$^{fl/fl}$ mutants (G), PN^{e} lacks innervation by MPC, while is innervated by SSC (arrow). **H**, *Ezh2*- and *Hox*-dependent genetic circuitry of intrinsic and extrinsic Unc5b/Ntn1 regulation.